



# Holistic plug-*n*-play autonomous solar system integration: a real-life small-scale demonstration—a practical approach

Asimina Dimara<sup>1,2</sup> · Christos Sougles<sup>1</sup> · Sotirios Athanasiou<sup>3</sup> · Konstantinos Grigoropoulos<sup>1</sup> · Panagiota Sfakianou<sup>1</sup> · Alexios Papaioannou<sup>1,4</sup> · Stelios Krinidis<sup>1,4</sup> · Dimitrios Triantafyllidis<sup>1</sup> · Ioannis Tzitzios<sup>1</sup> · Christos-Nikolaos Anagnostopoulos<sup>2</sup> · Aristoklis Karamanidis<sup>5</sup> · Vaia Saltagianni<sup>5</sup> · Dimosthenis Ioannidis<sup>1</sup> · Dimitrios Tzouvaras<sup>1</sup>

Received: 28 January 2023 / Accepted: 8 April 2023 / Published online: 11 May 2023  
© The Author(s) 2023

## Abstract

Autonomous PV systems offer a substitute for or a safety net against the transmission and distribution companies' rising and expanding electricity delivery fees. Across the world, delivery fees have climbed by about 3% annually while the cost of energy supply has only gone up by 5% over the past 15 years. In this paper, the drawbacks of PV system integration are highlighted while introducing a unique autonomous PV system. The system is also constructed in a reproducible way so that it can be duplicated. Replicability is showcased by the presentation of two separate PV systems that were created and evaluated using the same methodology. One system uses Si-based conventional photovoltaics, while the other uses dye-sensitized solar cells. The systems that are being offered also support remote connections, allowing all of the data from the PV system to be transmitted to a single endpoint (e.g., a visualization platform). Moreover, the system's batteries were modified to accommodate the two PV systems. Finally, experimental results showcase the operability of the proposed architecture.

**Keywords** Photovoltaic integration · Photovoltaic system · Interlinking · Remote connection · Interoperability · Data management

## 1 Introduction

As people become wealthier and richer and populations continue to increase, there is an increase in energy demand in almost all nations around the world. Over the course of more than 50 years, the world's energy consumption has risen almost every year [1]. Specifically, in 2021, the demand for primary energy increased by 5.8%, exceeding the levels of 2019 by 1.3%. Furthermore, the European Union (EU) imported almost 58% of the energy it consumed because its

---

✉ Asimina Dimara  
Dimara@aegean.gr

✉ Alexios Papaioannou  
alpapa@mst.ihu.gr

Christos Sougles  
chris.sougles@iti.gr

Sotirios Athanasiou  
s.athanasiou@sunlight.gr

Konstantinos Grigoropoulos  
grigokos@iti.gr

Panagiota Sfakianou  
sfakianou@iti.gr

Stelios Krinidis  
krinidis@iti.gr

Christos-Nikolaos Anagnostopoulos  
canag@aegean.gr

<sup>1</sup> Information Technologies Institute, Centre for Research and Technology Hellas (CERTH), 57001 Thessaloniki, Greece

<sup>2</sup> Department of Cultural Technology and Communication, Intelligent Systems Lab, University of the Aegean (UoA), 81100 Mytilene, Greece

<sup>3</sup> Sunlight Group Energy Storage Systems, 14564 Athens, Greece

<sup>4</sup> Management Science and Technology Department, International Hellenic University (IHU), 65404 Kavala, Greece

<sup>5</sup> Sunlight Group Energy Storage Systems, 67200 Neo Olvio, Greece

own production could only meet 42% of its daily needs [2]. As a result, the EU is more than half the energy dependent on the countries that import energy products, while being vulnerable to those that provide a large share of energy products (e.g., natural gas) such as Russia [2]. Any energy source that cannot run out and can be used indefinitely could be considered the best solution for the EU. Sustainable energy satisfies our need for energy without the requirement for renewal or replenishment and poses no threat of going bad or running out. This is why the best solution to worldwide energy demands is renewable energy.

Presently, the most widely known and used renewable energy sources are considered to be solar energy and wind energy, but there are other sources like hydro energy, tidal energy, geothermal energy, biomass energy, and others. Photovoltaic (PV) systems are driving the transformation of the sun's energy to power and converting it from DC to AC [3]. Integration of photovoltaic systems into a grid is of significant importance to mitigate energy consumption. There are many PV system integration technologies and each of them has various compatibility or interoperability issues and certain barriers [3]. Specifically, there are specific challenges in already implemented PV systems that have to be addressed before starting a new system's integration [3].

On the same basis, microgrids, which are small, autonomous grids that may operate independently of the main grid, have gained popularity as a viable way to improve the grid resilience and reliability [4]. The microgrid is connected to a number of distributed generation (DG) units. For the microgrid to operate more effectively, the connections between DG units must be appropriate. Maximum power transmission is managed by the power electronics that connect the microgrid and DG units. The primary function of power electronics is to capture the maximum amount of power from the sources while shielding it from load dynamics [5]. Nonetheless, the expensive cost of installation and the low conversion efficiency of PV modules are two of the critical downsides of PV systems [6].

A PV module is actually a nonlinear power source, and the output power it produces is influenced by the outside environment and shading [7]. The PV module must operate on its maximum power point (MPP) in order to maximize the efficiency of the PV system, necessitating the use of maximum power point tracking (MPPT) techniques. Maximum power point trackers (MPPTs) are crucial components of PV power systems because they increase the power output of a PV module under specific circumstances. The ability of the solar panel to produce electricity is essentially predicted by machine learning (ML) techniques [8]. But when the day is cloudy it could become unpredictable [9].

This paper introduces a novel autonomous PV system highlighting the downsides of PV system integration. Moreover, the system is built up in a replicable manner so that

it may be duplicated. Within this context, the presentation of two different PV systems that were designed and tested on the same basis is demonstrated. One system includes conventional PVs (i.e., Si), and the other system includes dye-sensitized solar cells (DSSCs). Furthermore, the presented systems support remote connection so that all the data from the PV system may be pushed to a single endpoint (e.g., a visualization platform). Finally, the batteries of the systems were customized to support the two PV systems.

The remainder of the paper is organized as follows: Sect. 2 analyzes the related work of all the distinct parts of a photovoltaic system. In Sect. 3, the methodology followed to build up the systems is presented. Experimental results are presented in Sect. 4, while conclusions are drawn in the final section.

## 2 Related work

### 2.1 Solar systems

The photoelectric effect on semiconductor materials is the basis of solar photovoltaic cells. This shows that, under some circumstances, a single electron in a substance can absorb a photon [10]. A crystalline solid known as a semiconductor is one in which bonded electrons (i.e., valence electrons) and free electrons (i.e., conduction electrons) are only permitted at certain energy values, separated by an energy gap that is forbidden [10]. The only atoms that can make up a flawless crystalline semiconductor are those that belong to its own net [10]. These atoms may only be of one kind, as in silicon (Si) or germanium (Ge), or they may only be of two types, as in gallium arsenide (GaAs) or cadmium telluride CdTe, or they may be part of even more complicated formulations, such as indium–gallium–arsenide (InGaAs)[10]. Si photovoltaic cells are one of the most used photovoltaic cells and play a fundamental role as they increase the efficiency of c-Si solar cells [11].

### 2.2 Storage systems

As mentioned in the previous paragraphs, due to the unpredictability of PV systems, energy storage systems (ESS) are needed to stabilize and control power flow toward a load or the grid. The most common energy storage systems used along photovoltaics are secondary stationary batteries with lead acid, lithium ion, nickel–metal hydride, and nickel–cadmium cell chemistries. Primary batteries cannot be used since they cannot be recharged so they are not suitable for the power fluctuations created by the PVs. Stationary applications are defined into 2 different categories: behind-the-meter (BTM) and front-of-the-meter (FTM). BTM includes residential commercial and industrial applications while

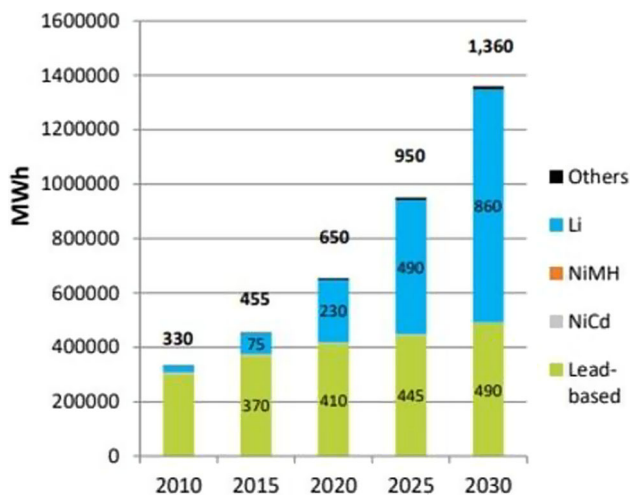


Fig. 1 Battery market demand [12]

FTM includes utility-scale applications. We are focusing on smaller applications so for the BTM case, where according to the EUROBAT Battery innovation road map, the prevailing technology is currently Li-ion batteries and will continue to be until 2030 with its percentage increasing compared to other types of chemistries.

Battery based small-scale PV systems can be used for example in cases of remote areas that are not connected to the national grid [13] to take advantage of favorable solar irradiance conditions for clean energy generation [14] and introducing prosumers that both produce and consume electricity to the power system to increase the system stability [15]. In the past, ESS applications have been investigated for smart grids and the systems were scaled down much more [16].

### 2.3 Solar system integration

Several researchers have studied the integration of solar systems into electricity grids and microgrids. In [17], the advantages and difficulties of integrating renewable energy sources, especially solar energy, into the electricity grid are presented. Also, the authors highlight the issue of perception by end users. Using various technical parameters related to electrical power quality, Salih et al. [18] analyzed the impact of integrating the solar system on the electrical distribution network and concluded that the integration of solar source with the load distribution grid can cause some errors. The authors of [19] also analyzed the impact of the integration of a solar PV system on an existing grid.

As depicted in Fig. 2, a centralized generation storage architecture is one in which the resources for generation (PV panels) and storage (batteries) are situated at a central position [20]. A central point with solar PV generation and storage provides with a one-way flow of power to a selected

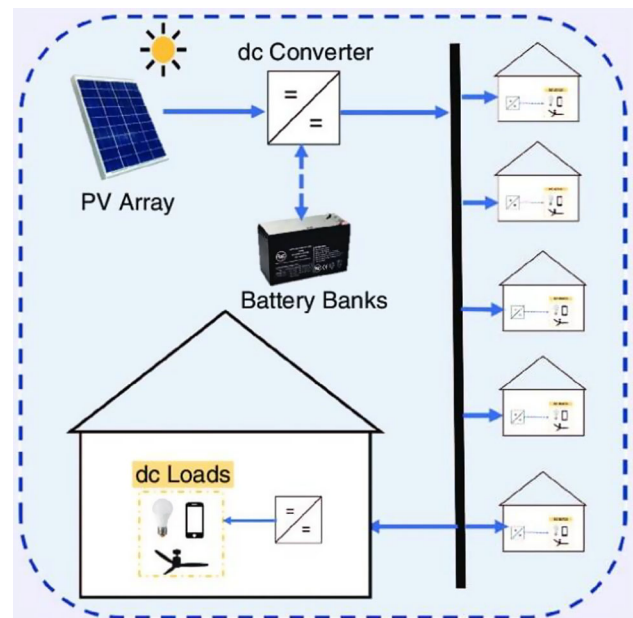


Fig. 2 Topological diagram of a typical centralized PV microgrid architecture [20]

load or a home. For the greatest power point tracking of PV output and stepping up the voltage to the microgrid distribution voltage level, a single DC–DC boost converter is needed. To step down the microgrid voltage level to the level needed for domestic equipment at the consumer end, another DC–DC converter is needed [20].

There are not any other research addressing two different PV system integration to the literature, to our knowledge. However, other PV system integration including DSSC PVs are presented in [21]. Also in [22], the state of colored photovoltaic panels today and their future prospects are discussed. Furthermore, in [23] on the basis of two years' worth of measurement data, a full-scale mock-up's power performance analysis of a transparent DSSC BIPV window is described. Finally, in [24], they introduce a di-carbazole-based dye as a potential sensitizer for dye-sensitized solar cells integrated with greenhouses.

## 3 Methodology

### 3.1 Solar systems

#### 3.1.1 Conventional photovoltaics

Silicon (Si) photovoltaic (PV) panels are the most dominant commercial technology of photovoltaic panels. Si PV panels are categorized into the following types [25]:

- Single-crystalline Si PV [26]. Photovoltaics of this type consist of large Si crystals with a width of around 300  $\mu\text{m}$ . Their efficiency is 13–18% and, therefore, their ability to produce large amounts of electric power by using small dimensions. This advantage makes them ideal for installation in spots where the dimensions are limited.
- Multi-crystalline Si PV [27]. Multi-crystalline Si PVs are manufactured with rods of melted and recrystallized silicon. For their construction, the rods are cut into thin pieces, by which the photovoltaic cells are produced. Their efficiency is 12–15%. For this reason, they require more space to produce the same amount of electric power compared to that for single crystalline. Their advantage is the low construction cost; therefore, they are ideal for installation in spots with no limited space.
- Formless Si PVs [28]. PVs of this type consist of a thin Si layer that is evenly placed on a suitable trestle. This trestle can be a variety of materials, from stiff to very flexible. For this reason, they can be installed on curved or flexible surfaces. Despite their high efficiency in absorbing light photons, their photovoltaic efficiency is much lower than that of crystalline, around 6%. However, they can be used in applications where high efficiency is not required because of their low construction cost, compared to that of crystalline.
- Hybrid high-efficiency Si PVs [29]. Hybrid PVs consist of single-crystalline Si covered by a thin layer of formlessness Si. The advantage of this type is the high efficiency (+18%), and the low-temperature factor giving them the capability to produce higher amounts of electric power and energy than another system with the same dimensions. The main disadvantage of this type is the high construction cost.

### 3.1.2 Dye-sensitized solar cell photovoltaics

SSC PV panels are a technology of thin and highly flexible PV panels. They consist of a transparent conductive layer, the electrode, which is oriented at to a radiation source [30]. A membrane semiconductor is placed on the electrode. The material used as a semiconductor is usually dioxide of titanium ( $\text{TiO}_2$ ). The surface of the semiconductor absorbs a layer of dye material, and an electrolyte is placed on another layer. When the molecules of this material absorb photons, electrons are transported to the conductive part of semiconductor. The dye material become neutral again with the replacement of lost electrons by the electrolyte. DSSC PV are very efficient to produced electric current by the photons that are absorbed by the  $\text{TiO}_2$ . Those photons are mainly part of red spectrum of visible radiation. For this reason, DSSC PV are less efficient under solar radiation and more efficient under night or vehicle lighting, than silicon PV. The

efficiency of DSSC is around 11% under solar radiation and 30% under radiation of red spectrum [30].

DSSC photovoltaic is an ideal option for installation on low-solar-radiation spots where electricity production is required, such as night lighting or tunnel lighting on highways. In addition, DSSC photovoltaic is a very good option for installations with solar radiation of curved surfaces when the required production of electricity is low.

The main disadvantage is that the electrolyte is extremely sensitive to temperature. At low temperatures, the electrolyte can freeze, halting the production of electricity and causing physical damage to the panel. Higher temperatures cause the electrolyte's liquid to expand, making sealing the panels a serious problem [30].

### 3.2 Underlying adjustable hardware components

The architecture of the system will be presented by analyzing the Hardware components of the various units and sub-modules that compose it. In addition, there will be a justification for the selection of each element selected in each unit and how it can be connected to the other elements of the remaining units, and its specifications will be presented. The identifiable parts are depicted in Fig. 3. To replicate all the systems, the upper level is the level that needs to be redefined in a new system by evaluating the system requirements. As it may be observed, the system design, methodology, and procedures used to produce the results are thoroughly documented and explained. This documentation is detailed enough to allow others to replicate the system's setup and produce the same results while ensuring stability as presented in the experimental results section. Furthermore standardized protocols and tools for data collection, processing, and analysis were used to ensure that the data are processed consistently and reduce the risk of errors or bias in the results.

The mode of operation of the charging regulator is as follows:

- The PV system is forced to produce the maximum possible power (MPPT) depending on the current weather conditions (i.e., temperature, radiation)
- When the energy produced by the photovoltaic system is greater than the energy consumed by the load, then the excess energy is used to charge the battery, without exceeding the limits of the maximum battery charge.
- When the energy produced by the photovoltaic system is less than the energy consumed by the load, then the remaining energy is covered by the battery, without exceeding the maximum discharge limits of the battery.

The values of the electrical parameters (i.e., current, voltage, power) of PVs, batteries, and loads are measured through various sensors and sent in analog form to the Raspberry PI

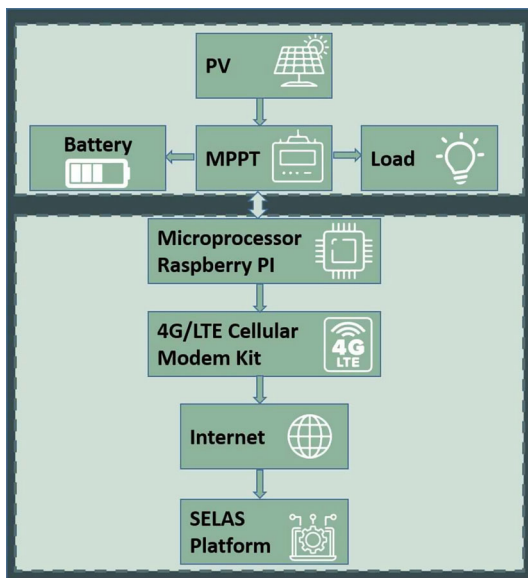


**Fig. 3** Underlying adjustable PV system components

(Rpi) controller. Then the controller adjusts the values of the electricity meters and through the 4G/LTE Cellular Modem Kit unit may be sent to an endpoint (e.g., platform of the proposed system (SELAS)). Finally, these values are processed, are analyzed, and can be visualized graphically through an appropriate interface (part of the SELAS platform).

### 3.3 Selection of the components

The underlying components of the selected system consist of the following components: MPPT, Pvs, batteries, and a load.

#### 3.3.1 Conventional PV system

The selection of the components was made as follows:

- i Initially, a load that should be fed by the system was selected. Its nominal capacity and consumption were determined over the course of a day. Specifically, selected as load:
  - One LED bulb with 5 Watt power.
  - The energy it consumes  $(5 * 24 \text{ h}) = 120 \text{ Wh}$  during a day.
- ii On the basis of the daily consumption of the load, the batteries were chosen so that when the production of the PVs is zero, they can supply the load for a period of approximately seven days. That is, the batteries should supply the following load: Load for 7 (days) \* 120 Wh = 840 Wh. Finally, based on the above needs, the battery was selected: 12 Volt and 96 Ah  $(12 \text{ V} * 96 \text{ Ah} = 1152 \text{ Wh} > 840 \text{ Wh})$

- iii The choice of the PV system was made so that their nominal power is sufficiently greater than the load, to be able to cover the needs of the load but also charge the battery. Based on the above estimations, the selection of photovoltaics is 5 Watts and 12 panels were used  $(5 * 12 = 60 \text{ W})$ .
- iv Based on the above, the choice of the MPPT-type charge regulator was made so that it can simultaneously support the PVs, the batteries, and the load.

#### 3.3.2 DSSC PV system

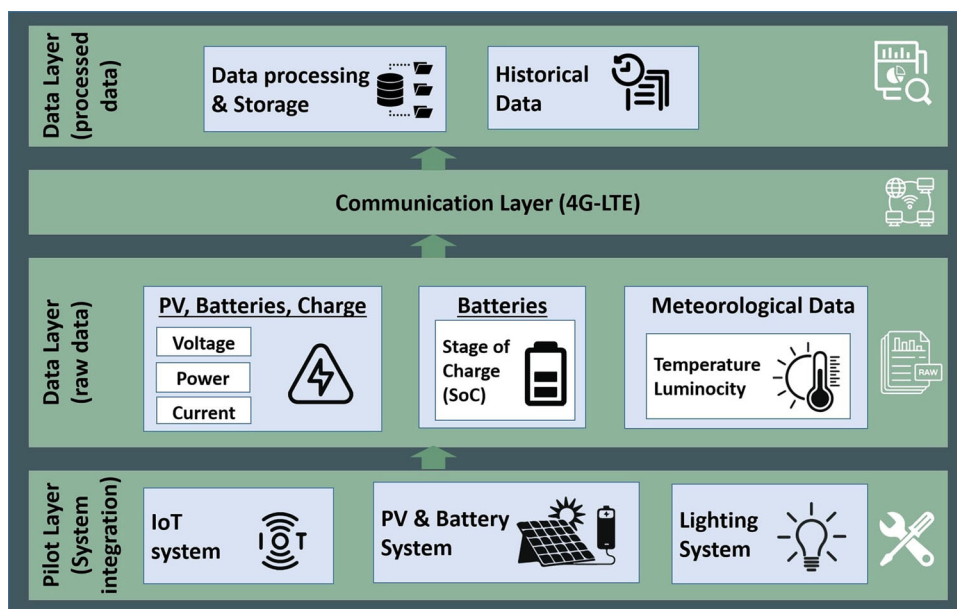
The selection of the components was made as follows:

- i A load that should be fed by the system was selected and its nominal capacity and consumption were determined over the course of a day. Specifically selected as load:
  - 6 Led lamps 40 mA at 3.3 Volt =  $(132 \text{ mW})$
  - The amount of energy consumed:  $(132 * 24 \text{ h}) = 3168 \text{ Wh}$  during the a day.
- ii Based on the daily consumption of the load, the batteries were selected so that when the production of the PV is zero, they can supply the load for a period of approximately 2.5 days. That is, the batteries should supply the following load: • Load for 2.5 (days) \* 3.168 Wh = 7.92 Wh Finally, based on the above needs, the battery was selected: 12 Volt and 2.5 Ah  $12 \text{ V} * 2.5 \text{ Ah} = 30 \text{ Wh} > 7.92 \text{ Wh}$ .
- iii The choice of the PV system was made so that their nominal power is sufficiently greater than the load to be able to cover the needs of the load but also charge the battery. Based on the above estimations, the selection of photovoltaics is 3 Watts and 4 panels  $(4 * 3.3 = 13.2 \text{ W}) > 132 \text{ mW}$ .
- iv Based on the above, the choice of the MPPT-type charge regulator was made so that it can simultaneously support the PVs, the batteries, and the load.

#### 3.4 Single-point platform integration

The system (SELAS) uses different communication and data transfer protocols, and basically, through the processors (i.e., Raspberry Pi Zero W and Raspberry Pi 4 G Module), it is able to push data from the various installed sensors (e.g., temperature, brightness, radiation, or sensors for measuring the prices of electricity units). All data streams are drawn from the SELAS platform, stored in its database, and then can be analyzed and used. All this information may be essentially visualized in various tabs.

**Fig. 4** Overall SELAS conceptual architecture



## 4 Experimental

In this particular chapter, the elements that make up the proposed system are presented and described, and then, the technical characteristics of each element selected are presented.

### 4.1 Conventional PV system

#### 4.1.1 Load

According to the previous descriptions, in which the method and order of selection of the energy source were analyzed and explained, the load to be used must first be determined. This, obviously, is quite logical, since the load that must be supplied is first estimated so that the combination of batteries and photovoltaics that will be installed can be defined in order to be able to supply it continuously so that we have an autonomous system. The technical features of the load used in the system of conventional PVs are presented in *T* (Fig. 5):

#### 4.1.2 Storage systems

The electrical accumulator (batteries) specifications should be determined after the load. This option is based on the fact that batteries are required to supply the load for some days when the production of photovoltaic is insufficient to keep the system operating autonomously. Therefore, based on the daily consumption of the load for the PV systems that were manufactured, different batteries were selected and are presented below in the respective sub-chapters.

In the case of the conventional PV system, the batteries were chosen so that when the generation of PV is zero, they

can supply the load for a period of approximately 7 days. Based on the above, the batteries should supply the following load:  $7(\text{days}) * 120 \text{ Wh} = 840 \text{ Wh}$ . Specifically, the capacity of the battery should be greater than 840 Wh so that when it is fully charged it can supply the load for at least seven days. The battery and the specifications selected are depicted in Fig. 6.

#### 4.1.3 PV cells

The photovoltaic frames used in the original system are 12 compatible silicon (Si) PVs. In the case of the conventional PVs, taking into account the nominal power of the load and the nominal energy of the batteries, the selection of the PV panels was made based on the following estimations: PV panel 5Watts and 12 PV frames were used, so the total power is  $5 * 12 = 60 \text{ W} \gg 5 \text{ Watt}$ . The PV cells and the specifications are depicted in Fig. 7.

#### 4.1.4 Charge controller

The controller selected in the system with the Si PV type was determined in such a way that the following criteria were met:

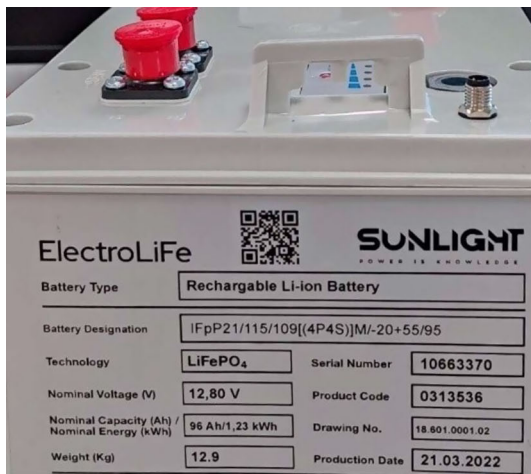
- Must support a battery with a nominal voltage of 12 V
- The nominal charging current should be smaller than the nominal charging current of the battery (25 A). The nominal charging current of  $10 \text{ A} < 25 \text{ A}$ .
- The temperature on the days of analysis at all periods of time should not exceed the operating temperatures of the controller. Indeed, the selected controller works satisfactorily at temperatures  $[-30 \text{ }^\circ\text{C}, 60 \text{ }^\circ\text{C}]$ , a range that does not disturb the temperatures on the 2-day cycle.

**Fig. 5** Load used for the conventional Pvs



Technical features of the load used in the system of conventional PVs

Type of load	Lamp
Nominal power	5 Watt
Daily consumption	(5*24h) = 120Wh



Battery specifications for the Conventional PVs

Type	Lithium-Ion battery
Technology	LiFeP04
Nominal Voltage	12.8 V
Capacity	96 Ah
Nominal power	(12.8V * 96Ah)/1.23 kWh
Nominal charging	96 A
Weight	12.9 Kg

**Fig. 6** Battery for the conventional system

**Fig. 7** Si PV panels



Technical features of the Si PV cells

Short circuit current	0.299
Current at maximum power (Impp)	0.278 A
Open circuit voltage	22.1 V
Maximum Power point Voltage (Vmpp)	18 V
Max power	5 W
Dimensions	260 x 200 x 17 mm
Weight	0.5 kg

- The maximum power that the controller can withstand from PVs is greater than that set for PVs [5 Watt \* 12 panel] = 60 W. And this criterion is satisfied as the maximum power that the controller can withstand is 145 Watt.
- The maximum voltage of PV that can be connected to the controller that will be selected is greater than the open-circuit voltage of PV (22.1 V). Specifically in this particular MPPT, PV can be connected with a voltage that does not exceed 75 V > 22.1 V.

Based on the above needs that have been identified and must be met by the controller that will be used, the Victron

BlueSolar controller was chosen for the compatible photovoltaics, which is shown in Fig. 8 along with its technical characteristics, which meet the requirements for the choice of the selected system above.

#### 4.1.5 Voltage and current sensors

The role of voltage and current sensors is to detect and convert the currents and voltages of the battery system, PV panels, and loads into analog signals. These signals are sent to the controller to be digitized. The charge–discharge controller used, the Victron BlueSolar, has built-in sensors to detect



Technical features of the charge controller

Battery voltage	12 V
Nominal charging current	10 A
Maximum PV Voltage	75 V
Maximum PV Power	145 W
Automatic load discharge	Yes, max 15
Maximum efficiency	98%
Self consumption	10mA
Continuous / Peak Load Current	15A/ 50A
Protections	Reverse battery polarity, Output short circuit
Operational Temperature	-30C to 60C
Dimensions	100 x 113 x 40 mm
Security	EN/IEC 62109

Fig. 8 Charge controller for the conventional system

Fig. 9 Load used for the DSSC Pvs



Technical features of the load used in the system of DSSCCS PVs

Type of load	6 Lamps
Nominal power	132 mW
Daily consumption	(132mW * 24hours) = 3.168 Wh

and convert the values of PV, load, and battery electrical quantities into analog signals, and there was no need to add an additional external sensor.

## 4.2 Dye-sensitized solar (DSSC) PV system

### 4.2.1 Load

According to the conventional PVs, the technical features of the load used in the system of DSSC PVs are presented in Fig. 9:

### 4.2.2 Storage systems

In the case of the DSSC-type PV systems, the batteries were chosen so that when the generation of PV is zero, they can supply the load for a period of approximately 2.5 days. Based on the above, the batteries should supply the following load:  $2.5(\text{days}) * 3.168 \text{ Wh} = 7.92 \text{ Wh}$ . The capacity of the battery should be greater than 7.92Wh so that when it is fully charged it can supply the load for at least two days. Finally, based on the above needs, a battery was selected: 3.6 Volt and 2.5 Ah,  $3.6\text{V} * 2.5 \text{ Ah} = 9 \text{ Wh} > 7.92 \text{ Wh}$ .

The battery and the specifications are depicted in Fig. 10.

### 4.2.3 PV cells

The photovoltaic frames used in the original system are 2 DSSC (dye-sensitized solar cell) printed by Brite Solar [31] during the SELAS project [32]. In the case of the DSSC-type PVs, taking into account the nominal power of the load and the nominal energy of the batteries, the selection of the PV panels was made based on the following estimations. PV panel 3.3Watts and 3 PV frames were used, so the total power is  $2 * 3.3 = 13.2 \text{ W} \gg 66 \text{ mW}$ . The PV cells and the specifications are depicted in Fig. 11

### 4.2.4 Charge controller

The controller selected for the system with the PV-type DSSC was determined in such a way that the following criteria were met:

- Charging current supply up to 2A in 3.7V lithium battery.
- The power of DSSC (2 panel \* 3.3 Watt) = 6.6 W do not exceed the maximum power that can be accepted by the MPPT.

The controller that was specified is therefore the DFR0535 of the DFROBOT company with MPPT (maximum power



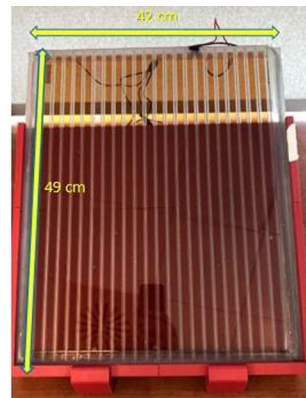
Fig. 10 Battery for the DSSC system



Battery specifications for the DSSC PVs

Type	Lithium Ion battery
Nominal Voltage	3.6 V
Capacity	2.5 Ah
Charge discharge	2A

Fig. 11 DSSC PV panels



Technical features of the DSSC PV cells

Short circuit current	0.299 A
Current at maximum power (Impp)	0.278 A
Open circuit voltage	22.1 V
Maximum Power point Voltage (Vmpp)	18 V
Max power	5 W
Dimensions	260 x 200 x 17 mm
Weight	0.5 kg

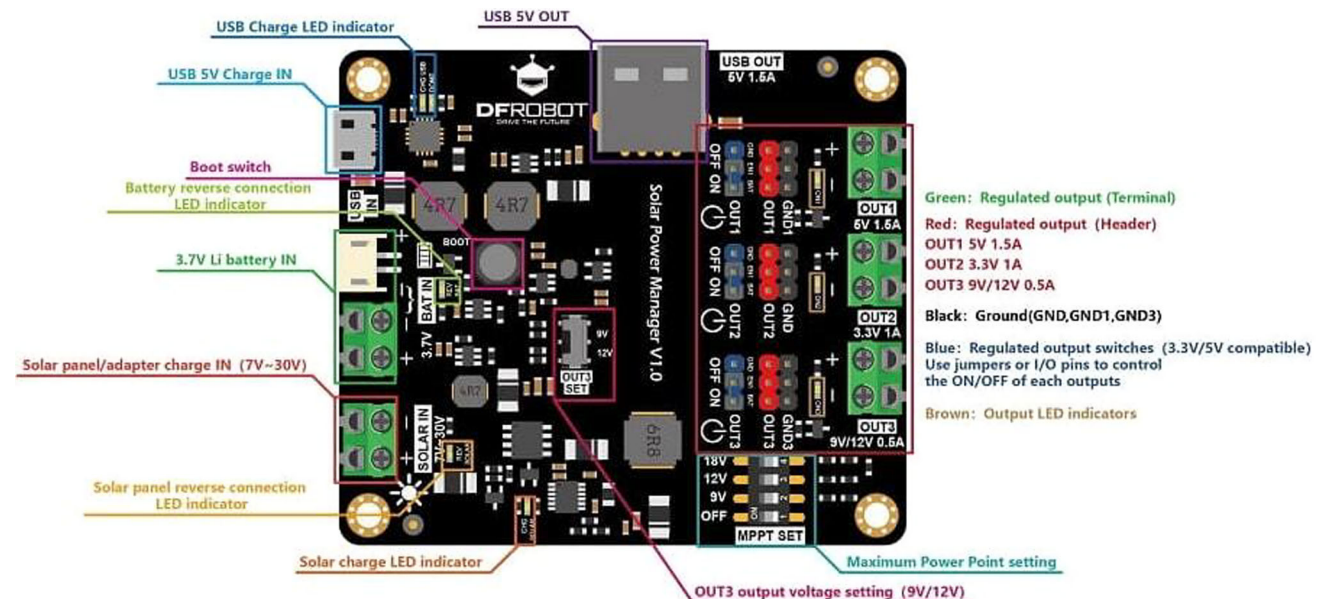


Fig. 12 Charge controller for the DSSC system

point tracking) technology. The charge controller and the specifications are depicted in Fig. 12 and Table 1.

#### 4.2.5 Voltage and current sensors

The sensor used in this case operates with four-channel monitoring via the I2C/SMBus interface, with a 0.1 Ω 1% sampling resistor bidirectional current measurement up to 3.2 A, built-in 12-bit ADC (multiple sequential conversion)—voltage measurement range 0 to 26V. In the image and the following table, the voltage and current sensor that was used and its characteristics can be visualized. The sensor and the specifications are depicted in Fig. 13.

### 4.3 Customized and adaptable storage systems

Based on the original requirements, batteries were customized for the system. The results are addressed in this chapter. Initial measurements were performed to characterize available cells and evaluate their performance. This was done to verify if they were a good fit to use for assembling the battery pack.

The cell under test rated voltage was 3.2 V, rated max constant current 24 A and the rated capacity is 24 Ah. As depicted in Fig. 14, when the cell discharges with 1 C (24 A) constant current, in 1 h we have a complete discharge of the cell as expected. At a rate of 0.5 C (12 A) constant current, there is a

**Table 1** Technical features of the charge controller

Solar power management IC	LTC3652
Solar input voltage	7–30 V
Maximum charge current (solar)	2 A (solar/USB)
Topology	DC–DC buck
Battery	3.7 V lithium battery
MPPT	9 V/12 V/18 V optional
Battery protections	Overcharge/overdischarge/overcurrent/reverse connection protections
Output protections	Short circuit/overcurrent/overheat protections
USB charge IN	Yes
USB OUT	5 V 1.5 A
Regulated OUT	Three regulated outputs 3.3 V 1 A, 5 V, 1.5 V, 9 V/12 V 0.5 A
Dimension	78.0 mm × 68.0 mm
Features	A complete multi-functional solar power management module. Applications: small solar street lamp, solar-powered robots for 9 V/12 V/18 V solar panels within 20 W

full discharge in 2 h. At a rate of 0.2 C, (4.8 A) a full discharge takes place in 5 h etc. In Fig. 15, the cell cycling process may be observed with its current, voltage and capacity plotted versus time. Both charging and discharging process consist of multiple steps: constant current (CC), constant voltage (CV) followed usually by a relaxation step. The results here verify the good behavior of the cell according to its specs.

In the case, the above cell for a 4P4S pack is used:

$$\begin{aligned}
 v_{\text{pack}} &= 4_s * 3.2 \text{ V} = 12.8 \text{ V} \\
 i_{\text{pack}} &= 4_p * 24 \text{ A} = 96 \text{ A} \\
 Q_{\text{pack}} &= 4_p * 24 \text{ Ah} = 96 \text{ Ah},
 \end{aligned}
 \tag{1}$$

where the subscript denotes whether the cells are in series or parallel. Based on the above, the pack assembled with the cell above provides  $12.8 \text{ V} * 96 \text{ Ah} = 1228 \text{ Wh} > 840 \text{ Wh}$  and the requirements are met successfully. In Fig. 16, images from the battery pack assembly are depicted.

Based on the above results (Figs. 14 and 15), a battery pack was made with the configuration 4P4S. This provided a battery pack with  $4 * 24 = 96 \text{ Ah}$  of capacity ( $Q$ ) and  $4 * 3.2 = 12.8 \text{ V}$  of voltage. In the image below, you can see the images from the battery pack assembly (Fig. 16).

### 4.4 Analog-to-digital signal controller

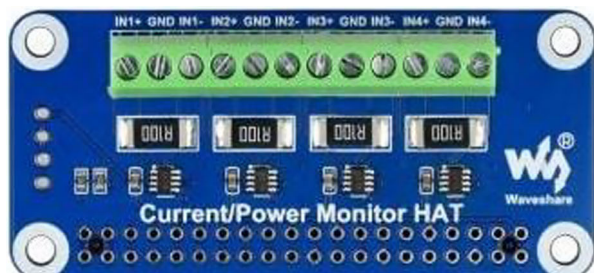
#### 4.4.1 Analog-to-digital signal controller WiFi connection

The controller used that supports a WiFi connection is the Raspberry Zero W (Fig. 17). The Raspberry Pi Zero W adds wireless LAN and Bluetooth connectivity to the Pi Zero line. The Raspberry Zero W specifications:

- 802.11 b/g/n wireless LAN
- Bluetooth 4.1
- Bluetooth low energy (BLE) 1GHz, single-core CPU 512MB RAM
- Mini HDMI port and micro USB On-The-Go (OTG) port Micro USB power HAT-compatible
- 40-pin header Composite video and reset headers CSI camera connector

#### 4.4.2 Analog-to-digital signal controller remote connection 4 G

Raspberry Pi 4-4 G Module (Fig. 18) provides a Modem Kit for the Raspberry Pi with which the Internet can be accessed with mobile data without requiring a WiFi connection. Essentially, it is possible to set up the Raspberry Pi as a remote web server accessing the Internet to remote locations worldwide. Note that the Raspberry is connected to the charge–discharge controllers with a USB port.



Technical features of the Sensor

Operating voltage	3.3V /5V
Voltage Range	[0, 26] V
Current Range	[-3.2 , 3.2] A
Dimensions	65mm x 30mm

**Fig. 13** Voltage and current sensor for the DSSC system

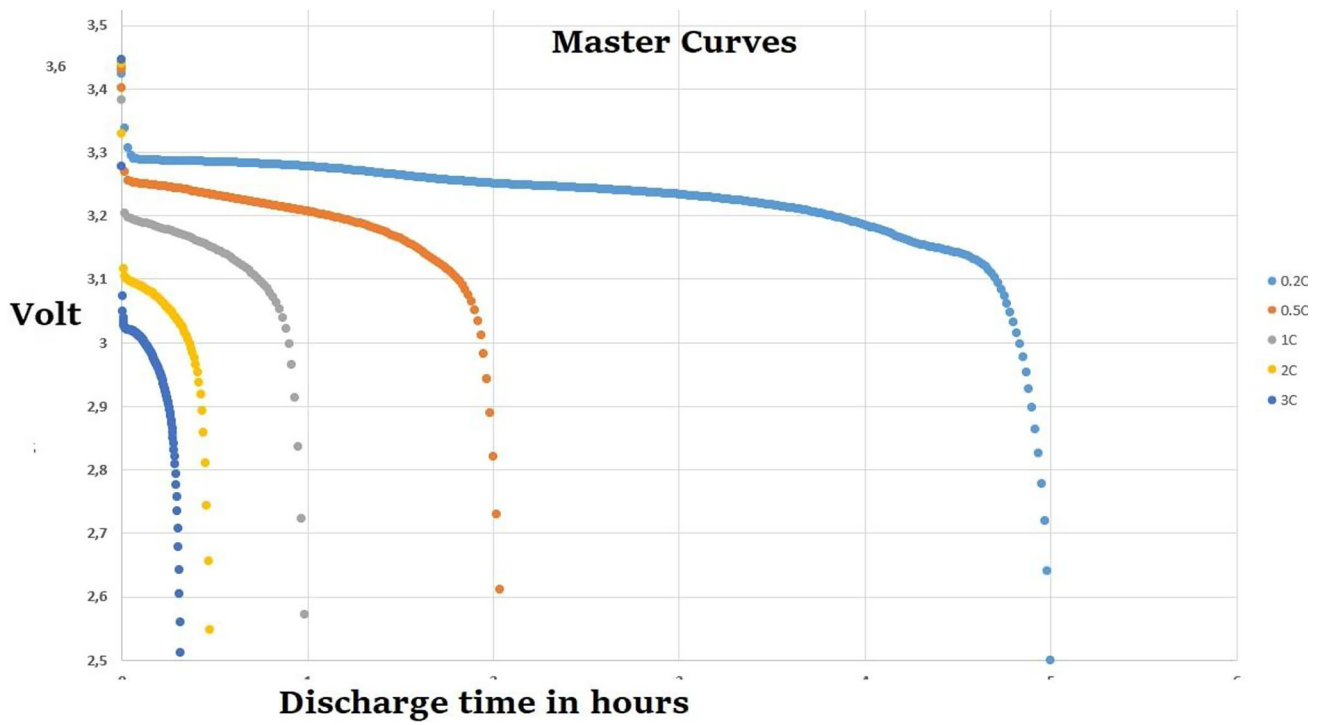


Fig. 14 Master curve versus discharge time

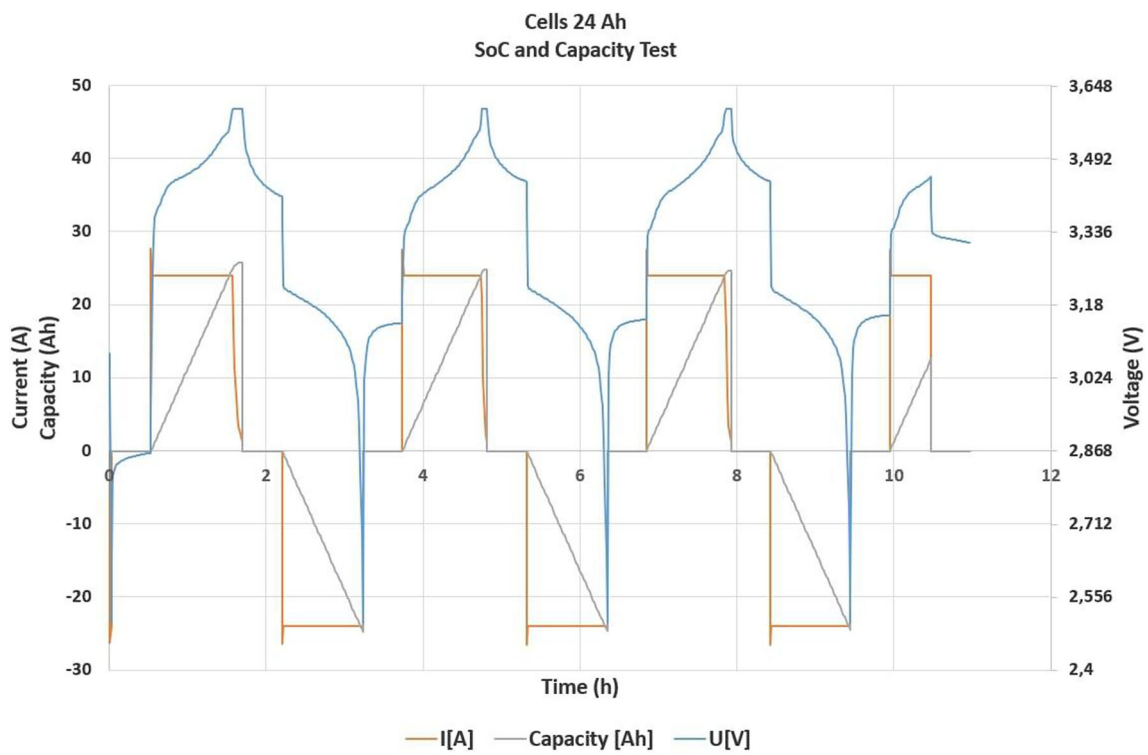


Fig. 15 SoC and capacity test

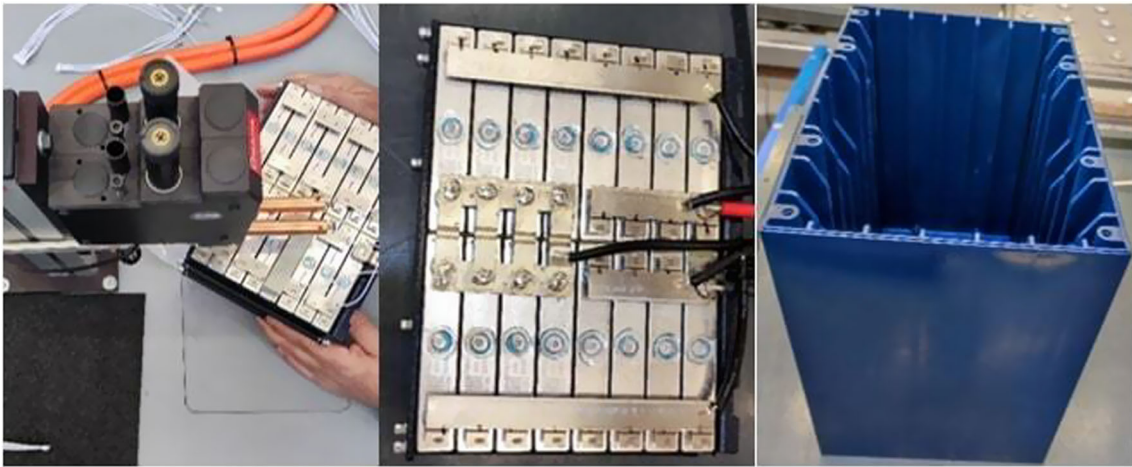


Fig. 16 Assembly of the battery pack

Fig. 17 Raspberry zero W

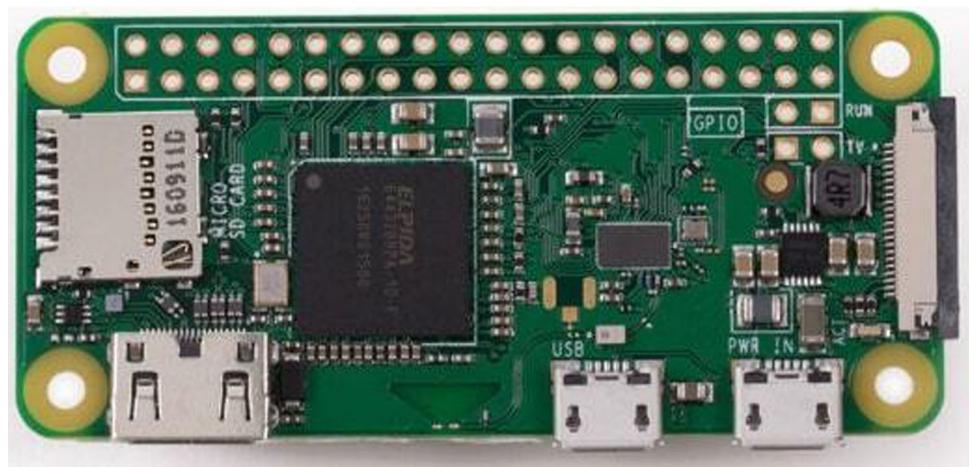
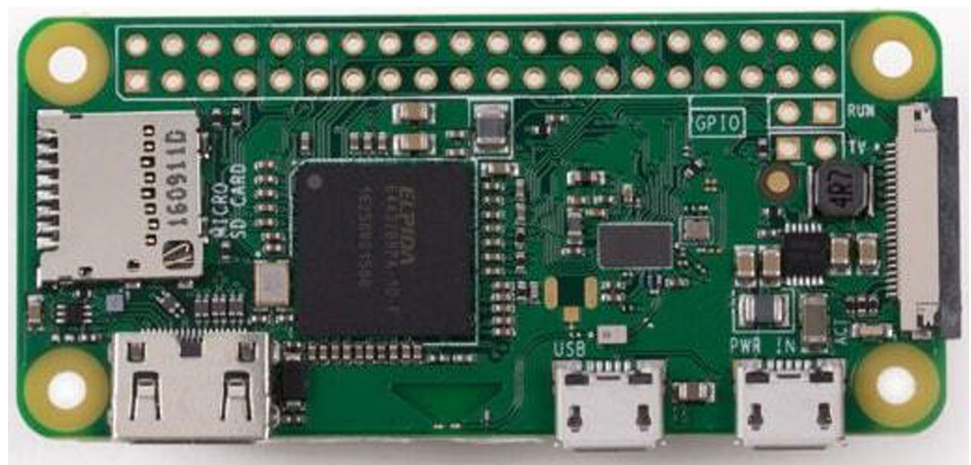


Fig. 18 Raspberry Pi 4-4G



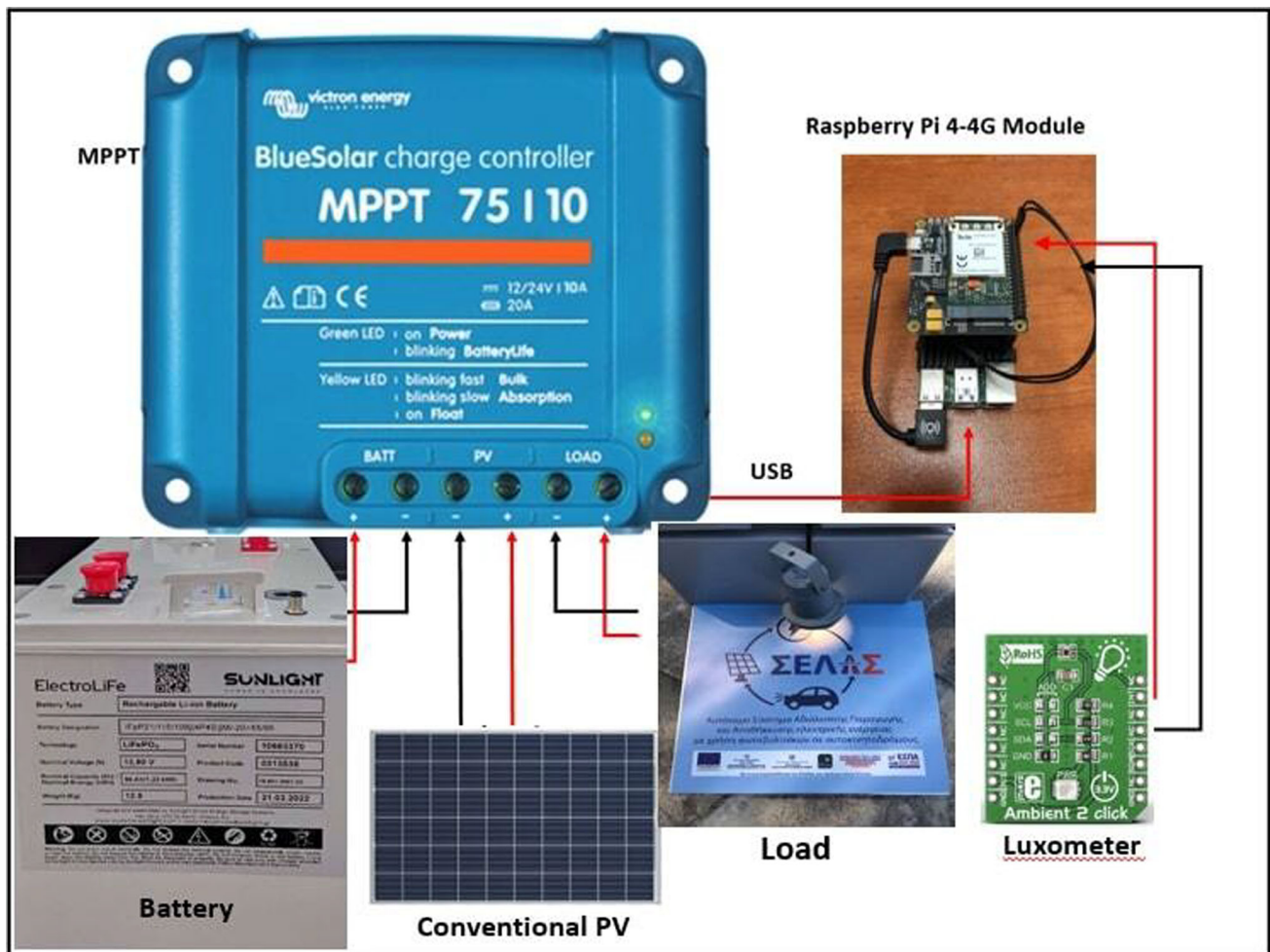


Fig. 19 Overall system architecture

## 4.5 Overall system architecture

### 4.5.1 Conventional PV system

The overall conceptual architecture of the conventional PV system as described above is depicted in Fig. 19.

It must be noted that the remote connection in a PV system integration is of ultimate important for several and various reasons. To begin with, remote connection allows for real-time monitoring and control of the PV system, regardless of its physical location. This enables operators to monitor the system’s performance, detect faults or issues, and take corrective action in a timely manner, which can improve the overall performance of the system. Moreover, remote connection can also improve the efficiency of PV system operations. For example, remote monitoring can help operators optimize the system’s energy production and reduce downtime, while remote control can help operators adjust the system’s settings to maximize energy generation. Finally, the remote connection can facilitate the scalability of PV systems. Operators

can monitor and control multiple systems from a central location, making it easier to manage and expand large-scale PV installations.

### 4.5.2 Dye-sensitized solar PV system

The overall conceptual architecture of the DSSC PV system as described above is depicted in Fig. 20.

## 4.6 Overall system laboratory tests

### 4.6.1 Conventional PV system

As part of laboratory tests, photovoltaics were placed outside the offices of CERTH premises and specific values were tested (Fig. 21).

In Figs. 22 and 23, the power and current of the PV systems as measured and pushed to SELAS platform is depicted. Certain fluctuations may be observed in the current produced by PV due to shading because of clouds.

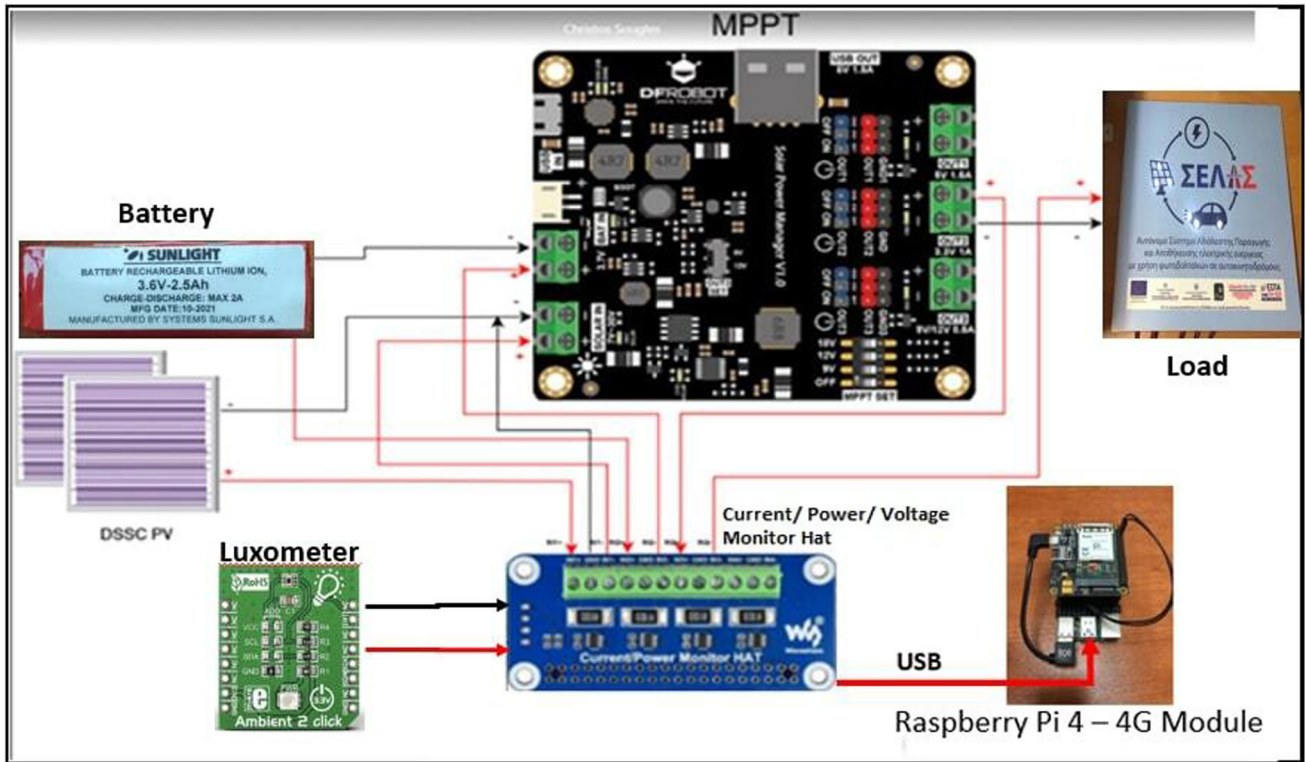
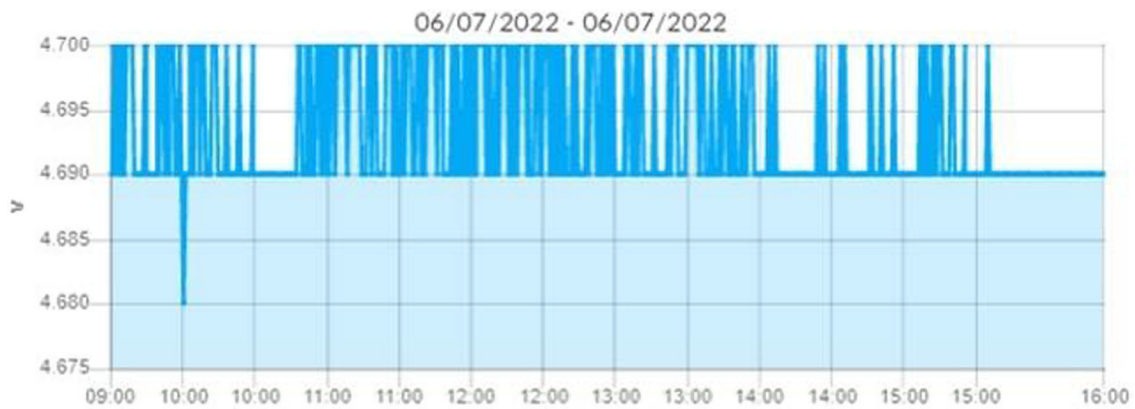


Fig. 20 Overall system architecture

Fig. 21 Conventional PV system laboratory tests





**Fig. 22** Conventional PV system laboratory tests: PV voltage values

**Fig. 23** Conventional PV system laboratory tests: PV power values



In Figs. 24 and 25, the power and current of the battery are presented. As it may be observed in the charts of the voltage and current of the battery, from 13:00 to 15:00 the battery is discharged due to covering the needs of the load. After 15:00, the energy supply from the PV to the battery is observed which is in compliant with the PV operation charts.

#### 4.6.2 Dye-sensitized solar PV system

The DSSC system was tested and showcased during a workshop of the SELAS project (Fig. 26). The system was tested by placing DSSC photovoltaics inside the central building of CERTH and values were gathered. The system was placed near the window without the PVs having direct sunlight exposure. The point was chosen in order to evaluate the performance of the system in low-light conditions.

Figures 27 and 28 show that in DSSC photovoltaics, there are peaks in the curves of their electrical quantities. This is due to the fact that DSSC photovoltaics are more sensitive than conventional ones. Specifically, they are more sensitive to other wavelengths of light (except solar) and therefore produce strong peaks (positive or negative) when a lot of radiation falls on them. It is also noticed that the current, with which the PV feeds the system increases as the external lighting becomes more intense due to the sunshine. The price

of electricity reaches its maximum point between 13:00 and 15:00.

Figures 29 and 30 show that the battery consumption is meeting the needs of the load, since the peaks in current consumption coincide with those of the load. Moreover, it may be noticed that the PVs are operating with current and power much smaller than the maximum (MPPT modulation). This is because the system is self-contained, the battery is fully charged, and the load's energy requirements are much less than the energy produced by the PVs in MPPT mode. The inverter, therefore, forces the PVs to produce enough power to safely supply the load.

## 5 Conclusion

Microgrids, are compact, self-sufficient grids that can function apart from the main grid. The distributed generation (DG) units are linked to the microgrid. The connections between the DG units must be appropriate for the microgrid to function more efficiently. The power electronics that link the microgrid and DG units control the maximum power transfer. Capturing the most power possible from the sources while protecting it from load dynamics is the main goal of power electronics.

**Fig. 24** Conventional PV system laboratory tests: battery current values



**Fig. 25** Conventional PV system laboratory tests: battery power values



**Fig. 26** DSSC PV system laboratory tests



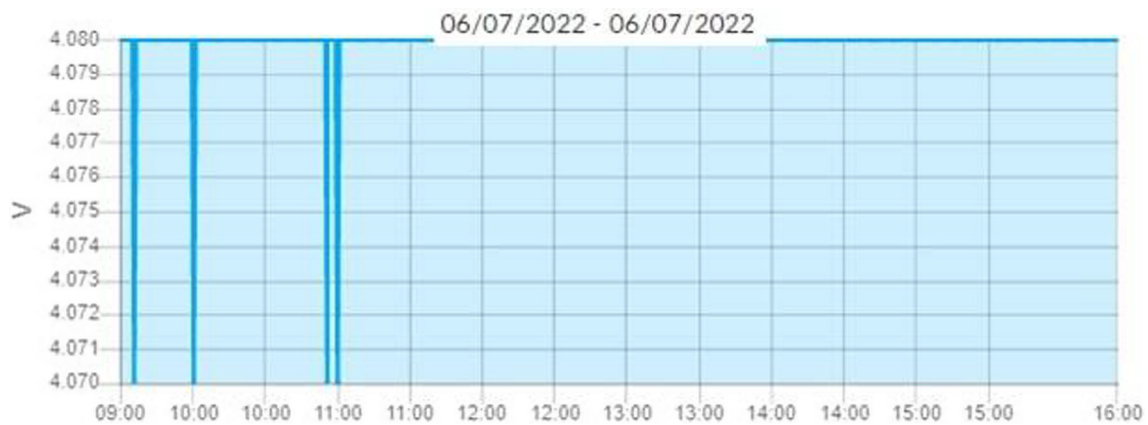


**Fig. 27** DSSC PV system laboratory tests: PV voltage values

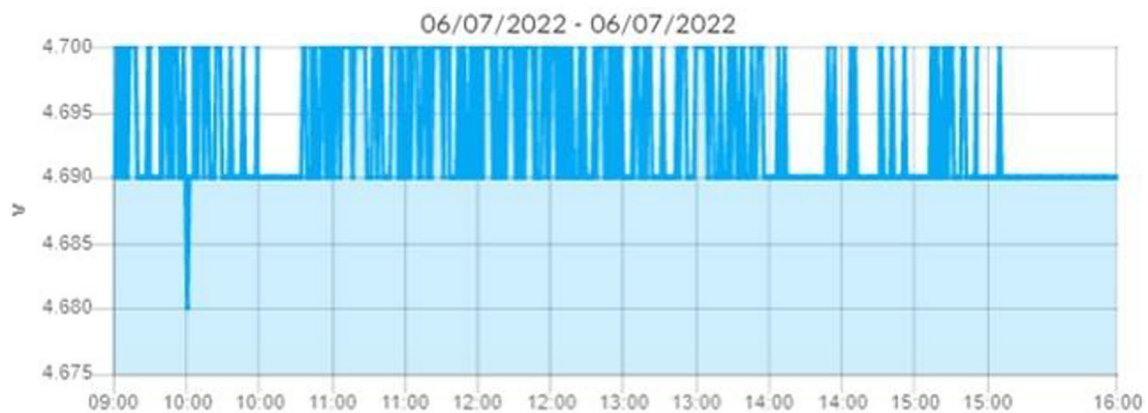


**Fig. 28** DSSC PV system laboratory tests: PV power values

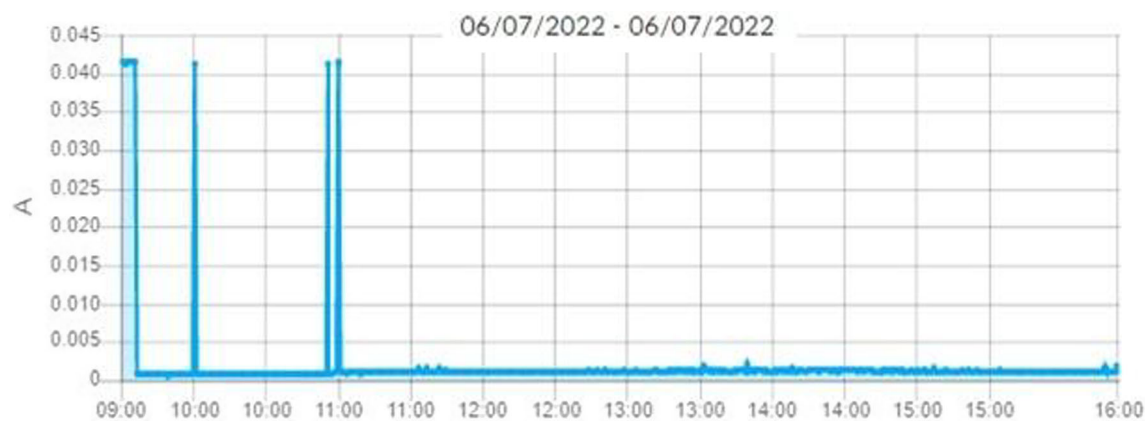


**Fig. 29** DS PV system laboratory tests: battery electric current values

This article highlights the drawbacks of PV system integration while introducing a unique autonomous PV system. In order to be replicated, the system is also constructed in a repeatable manner. In this context, two distinct PV systems that were created and evaluated using the same methodology are presented. Si-based conventional PVs are used in one system, whereas dye-sensitive solar cells are used in the other

(DSSC). Additionally, the systems presented provide remote connections, allowing for the push of all PV system data to a single endpoint (e.g., a visualization platform). The system's batteries were finally modified to handle the two photovoltaic systems.

Through a variety of sensors, the electrical characteristics (current, voltage, and power) of PVs, batteries, and loads are

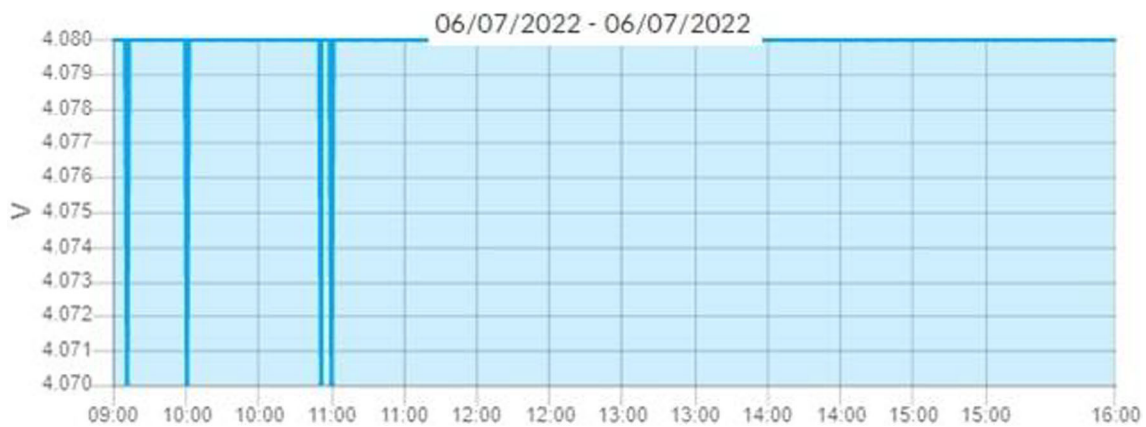


**Fig. 30** DS PV system laboratory tests: battery voltage values

measured and supplied to the Raspberry PI (Rpi) controller in analog form. The controller then modifies the readings on the power meters before sending them, for example, to the system's platform (SELAS), using the 4G/LTE Cellular Modem Kit unit. Finally, using an appropriate interface, these values are processed, examined, and made pictorial (part of the SELAS platform). Different batteries were used to the system because they have different energy storage needs and requirements. The type of battery used in a PV system will depend on factors such as the size of the system, the amount of energy storage needed, and the system's intended use. Furthermore, the replicable solution suggested is operable because it can be easily and consistently implemented in different settings and environments, producing similar results each time it is implemented. The SELAS solution provides a clear and detailed methodology for achieving a specific goal or solving a problem. This methodology can be documented and shared with others, who can then replicate the solution in their own settings.

Future work includes more tests in both a laboratory and field environment. In addition, AI algorithms will be integrated to monitor the stability of the system while preventing downtime of the PV system.

**Acknowledgements** This work is partially supported by the SELAS project co-financed by the European Regional Development Fund of the European Union and the Greek national funds through the Operational Program Competitiveness, Entrepreneurship and Innovation, under the call RESEARCH-CREATE-INNOVATE (Project Code:T1EDK-03547). The authors would also like to thank Symeon Parcharidis as well as the testing and prototyping laboratory of Sunlight Group, and Brite Solars for printing the DSSC PVs.

**Author Contributions** All authors contributed equally and reviewed the manuscript.

**Funding** Open access funding provided by HEAL-Link Greece. Not applicable.

**Data availability** Not applicable.

## Declarations

**Conflict of interest** Not applicable.

**Ethical approval** Not applicable.

**Open Access** This article is licensed under a Creative Commons Attribution 4.0 International License, which permits use, sharing, adaptation, distribution and reproduction in any medium or format, as long as you give appropriate credit to the original author(s) and the source, provide a link to the Creative Commons licence, and indicate if changes were made. The images or other third party material in this article are included in the article's Creative Commons licence, unless indicated otherwise in a credit line to the material. If material is not included in the article's Creative Commons licence and your intended use is not permitted by statutory regulation or exceeds the permitted use, you will need to obtain permission directly from the copyright holder. To view a copy of this licence, visit <http://creativecommons.org/licenses/by/4.0/>.

## References

1. How is global energy consumption changing year-to-year? <https://ourworldindata.org/energy-production-consumption>. Accessed 11 Nov 2022
2. EUROATAT: The EU imported 58% of its energy in 2020. <https://ec.europa.eu/eurostat/web/products-eurostat-news/-/ddn-20220328-2>. Accessed 07 Dec 2022
3. Nwaigwe KN, Mutabilwa P, Dintwa E (2019) An overview of solar power (PV systems) integration into electricity grids. *Mater Scier Energy Technol* 2(3):629–633
4. Kroposki B et al (2020) Autonomous energy grids: Controlling the future grid with large amounts of distributed energy resources. *IEEE Power Energy Mag* 18(6):37–46
5. Shafiullah G, Oo AM, Ali AS, Wolfs P (2013) Potential challenges of integrating large-scale wind energy into the power grid—a review. *Renew Sustain Energy Rev* 20:306–321
6. Hanane Y, Elhassan A (2017) A robust sliding mode MPPT controller applied to a stand-alone photovoltaic system. In: *Proceeding of the 33rd European photovoltaic solar energy conference and exhibition, Amsterdam*, pp 2201–2206

7. Yatimi H, Ouberrri Y, Aroudani E (2019) Enhancement of power production of an autonomous PV system based on robust MPPT technique. *Proc Manuf* 32:397–404
8. Salamanis AI et al (2020) Benchmark comparison of analytical, data-based and hybrid models for multi-step short-term photovoltaic power generation forecasting. *Energies* 13(22):5978
9. Badal FR et al (2019) A survey on control issues in renewable energy integration and microgrid. *Protect Control Mod Power Syst* 4(1):1–27
10. Hernández-Callejo L, Gallardo-Saavedra S, Alonso-Gómez V (2019) A review of photovoltaic systems: design, operation and maintenance. *Sol Energy* 188:426–440
11. Allen TG et al (2019) Passivating contacts for crystalline silicon solar cells. *Nat Energy* 4(11):914–928
12. Avicenne study: “EU battery demand and supply (2019–2030) in a global context” shows that in the next decade lead and lithium batteries are critical to clean energy transition
13. Perumal P et al (2020) Experimental setup for a battery based small-scale domestic PV system. In: *IEEE PES/IAS Power Africa*
14. Analyzing the operation of residential photovoltaic battery storage systems in Cyprus. N. G. Chatzigeorgiou et al, *The 12th Mediterranean Conference on Power Generation, Transmission, Distribution and Energy Conversion (MEDPOWER 2020)*
15. Ahmed A, Etherden N (2021) The potential for balancing the Swedish power grid with residential home batteries. In: *CIREED 2021—the 26th international conference and exhibition on electricity distribution*
16. Zyglakis et al (2021) Energy storage systems in residential applications for optimised economic operation: design and experimental validation. In: *2021 IEEE PES Innovative Smart Grid Technologies-Asia (ISGT Asia)*
17. Zahedi A (2011) A review of drivers, benefits, and challenges in integrating renewable energy sources into electricity grid. *Renew Sustain Energy Rev* 15(9):4775–4779
18. Salih ZH, Hasan GT, Mohammed MA, Klib MAS, Ali AH, Ibrahim RA (2019) Study the effect of integrating the solar energy source on stability of electrical distribution system. In: *2019 22nd International conference on control systems and computer science (CSCS)*. IEEE, pp 443–447
19. Dhlamini N, Chowdhury SD (2018) Solar photovoltaic generation and its integration impact on the existing power grid. In: *2018 IEEE PES/IAS PowerAfrica*. IEEE, pp 710–715
20. Nasir M et al (2018) Scalable solar dc micrigrids: on the path to revolutionizing the electrification architecture of developing communities. *IEEE Electr Mag* 6(4):63–72
21. Ghosh A (2020) Potential of building integrated and attached/applied photovoltaic (BIPV/BAPV) for adaptive less energy-hungry building’s skin: a comprehensive review. *J Clean Prod* 276:123343
22. Lee H, Song H-J (2021) Current status and perspective of colored photovoltaic modules. *Wiley Interdiscip Rev Energy Environ* 10(6):e403
23. Lee HM, Jong HY (2018) Power performance analysis of a transparent DSSC BIPV window based on 2 year measurement data in a full-scale mock-up. *Appl Energy* 225:1013–1021
24. Chalkias DA et al (2021) A di-carbazole-based dye as a potential sensitizer for greenhouse-integrated dye-sensitized solar cells. *Energies* 14(4):1159
25. Liang TS et al (2019) A review of crystalline silicon bifacial photovoltaic performance characterisation and simulation. *Energy Environ Sci* 12(1):116–148
26. Pilioungine M et al (2021) Analysis of the degradation of single-crystalline silicon modules after 21 years of operation. *Progress Photovolt Res Appl* 29(8):907–919
27. Kwembur IM et al (2020) Detection of potential induced degradation in mono and multi-crystalline silicon photovoltaic modules. *Phys B Condens Matter* 581:411938
28. Karthik R, Praveenkumar M, Thirunavukarasu P, Mohamed Thameemul Ansari A (2019) Study of online variable topology based photovoltaic grid-connected inverter
29. Park Y et al (2020) Effect of net voltage of thermoelectric generator on performance of hybrid energy device. *Energy Rep* 6:2836–2840
30. Omar A, Mohd SA, Nasrudin AR (2020) Electron transport properties analysis of titanium dioxide dye-sensitized solar cells (TiO<sub>2</sub>-DSSCs) based natural dyes using electrochemical impedance spectroscopy concept: a review. *Solar Energy* 207:1088–1121
31. BRITE SOLAR Solar Technologies. <https://www.britesolar.com/>. Accessed 28 Dec 2022
32. SELAS project. <https://www.iti.gr/iti/projects/.html>. Accessed 28 Dec 2022

**Publisher’s Note** Springer Nature remains neutral with regard to jurisdictional claims in published maps and institutional affiliations.